JOURNAL OF CATALYSIS 106, 216–234 (1987)

An *in Situ* X-Ray Diffraction Study of the Activation and Performance of Methanol Synthesis Catalysts Derived from Rare Earth–Copper Alloys

ROGER M. NIX, TREVOR RAYMENT, RICHARD M. LAMBERT,[1] J. ROBERT JENNINGS,* AND GEOFFREY OWEN†

*Department of Physical Chemistry, University of Cambridge, Cambridge CB2 1EP, England; *ICI Agricultural Division, P.O. Box 1, Billingham TS23 1LB, England; and †ICI New Science Group, P.O. Box 11, The Heath, Runcorn WA7 4QE, England*

Received December 3, 1986; revised February 9, 1987

The activation of NdCu, $NdCu_2$, $NdCu_5$, and $CeCu_2$ alloy precursors for methanol synthesis catalysts has been investigated by *in situ* XRD observations and concurrent measurements of methanol activity. Pressures of 2–30 bar and temperatures in the range 300–573 K were employed. It is shown that the formation of certain intermediate hydride phases is crucial to the eventual production of highly active catalysts and that methanol activity does *not* correlate with Cu crystallite size. CO_2 is a very effective poison which does not visibly affect the morphology of the metal phase. These findings strongly suggest that the reaction mechanism which obtains here is quite different from that which operates on conventional Cu–ZnO/Al_2O_3 methanol synthesis catalysts.

INTRODUCTION

Although *ex situ* or "post mortem" studies of practical catalysts are capable of yielding useful information about the relationship between structure and reactivity, the application of *in situ* physical methods offers the possibility of major progress in this field. The power of *in situ* X-ray diffraction (XRD) methods has recently been demonstrated in this laboratory (*1, 2*), and the present paper extends this approach to an investigation of the structural chemistry underlying the activation of a novel type of methanol synthesis catalyst. In addition to XRD measurements on the solid phases which evolve during activation of the alloy catalyst precursor and in the poisoning of the final active material, we report on the results of simultaneous measurements of methanol synthesis rates as the catalyst activates, stabilizes, and decays. Previously undetected hydride phases are shown to be crucial intermediates in the genesis of highly active catalysts, and the observed lack of correlation between Cu crystallite surface area and methanol activity provides important clues as to the nature of the active site. It appears that the catalytic reaction mechanism which operates here is quite different from that which obtains in the case of conventional methanol synthesis catalysts.

Intermetallic compounds of copper with various rare earth (RE) and actinide metals have been shown to be precursors to highly active, low temperature methanol synthesis catalysts (*3, 4*). Activation of the alloy starting material is accomplished in a synthesis gas feed under similar conditions of temperature, pressure, and flow to those employed during methanol synthesis (*4–6*). Discharged catalysts have been characterised by a variety of techniques including X-ray diffraction, SEM, TEM, DTA, and SIMS (*5–7*), yielding results consistent with the presence of only two bulk phases, namely, elemental copper and RE oxide.

[1] To whom correspondence should be addressed.

0021-9517/87 $3.00

Scarcely any work, however, has been reported on the mechanism of catalyst genesis from the intermetallic precursor despite abundant evidence that the ultimate activity is critically dependent on the activation procedure. In view of the extreme air-sensitivity of the materials concerned, a reliable, detailed investigation of this process can be accomplished only by employing *in situ* techniques of characterization. In this paper, we present the results of a controlled atmosphere X-ray diffraction study of the genesis, reactive behavior, and deactivation of the intermetallic-derived catalysts. The issues to be addressed reflect the initial aims of the work which were to determine:

(a) how the catalytic activity of the activated intermetallic is influenced by the chemical and physical properties of the starting alloy;

(b) the effect of temperature and pressure on the evolution of an active catalyst from precursor alloy and the nature and role of any intermediates in this process;

(c) the phases present in the activated catalyst and, more specifically, the identity of the catalytically active species; and

(d) the mechanism of catalyst deactivation and poisoning.

We report here work caried out on the activation of binary Nd–Cu alloys (NdCu, $NdCu_2$, $NdCu_5$) and Ce–Cu alloys ($CeCu_2$) in synthesis gas at pressures of 2–30 bar (1 bar = 10^5 Pa).

EXPERIMENTAL

X-ray diffraction patterns were obtained with a Siemens D500 diffractometer using Cu K_α radiation and a scintillation counter (SC) or position sensitive detector (PSD). The latter greatly enhances the rate at which data can be collected and, hence, allows the acquisition of more detailed kinetic results without interruption of the reaction conditions or, more generally, an improvement in signal-to-noise for a fixed scan rate.

A purpose-built sample cell capable of operating at pressures up to 50 bar and temperatures of 700 K was utilized in the experiments. A detailed description of the cell is to be published elsewhere (*9*) but its essential features are illustrated in Fig. 1. The sample is retained on an aluminum holder within a pressure vessel machined from solid beryllium. The reactant gases flow over the catalyst charge which is heated by conduction from a cartridge heater, the temperature being measured and controlled using a thermocouple fixed into the copper support block.

The intermetallic samples used in this work were prepared by electron-beam melting of the constituent metals under high vacuum, with subsequent annealing in an evacuated quartz ampoule for 4 weeks at 673 K or 3 weeks at 773 K. In each individual run a catalyst charge of 0.10–0.25 g was crushed to a particle size of 50–250 μm and loaded into the high-pressure cell under an argon atmosphere. The sealed cell was then transferred to the diffractometer and flushed out with high purity (99.995%) helium at room temperature while alignment was carried out. Using this procedure, no bulk oxidation of the samples prior to activation could be detected by XRD (the sampling depth for $NdCu_2$ is 0.5–1.8 μm over the 2θ range of 20–80° studied).

Reactant gases were obtained from BOC Ltd. (Special Gases) and used without further purification: hydrogen (CP grade: >99.999% pure), premixed CO/H_2

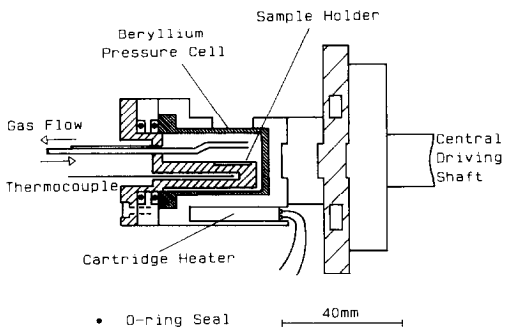

FIG. 1. High-pressure X-ray diffraction (XRD) cell (thermal insulation not shown for clarity).

(33 : 67—impurities $O_2 < 5$ ppm, $H_2O < 2$ ppm, and $CO_2 < 20$ ppm), premixed CO/CO_2/H_2 (32 : 2 : 64—impurities $O_2 < 3$ ppm and $H_2O < 10$ ppm), oxygen, and carbon monoxide (Research grade).

In most of the experiments reported, the effluent gas from the reactor/sample cell was monitored using on-line GC analysis. Molecular sieve 13X and Porapak N columns in a series/by-pass configuration were employed to separate the components and hence to correlate the methanol synthesis activity with the structural data obtained concurrently from the diffraction patterns. Standard flow rates of 50 cm^3 (STP)/min and 80 cm^3 (STP)/min at 15-bar total pressure were used for the Nd- and Ce-intermetallic experiments, respectively. Under these conditions, with the precursor charges and reactor temperatures employed, conversions were sufficiently low that the methanol yield determined may be taken to be directly proportional to the initial rate. [Note. We do not consider gas hourly space velocity (GHSV) to be a meaningful quantity in view of the variable expansion occurring upon activation (see below) and the flow conditions envisaged for this type of reactor cell (internal volume 4.4 cm^3).] In the case of treatment in pure hydrogen, however, the flow rate was generally reduced to zero once the reactor had attained a steady temperature and any outgassing that might have occurred during heating had ceased.

The major technical problem encountered in this study was the massive expansion which the sample undergoes during the activation process. The consequence of this expansion, particularly acute for the low Cu-content precursors, was a change in the sample diffraction plane and a gradual shift in the peak positions to higher 2θ as a result of the loss of vertical alignment. In addition, the peak shift was accompanied by a reduction in the scattered X-ray intensity as the gap between the sample surface and a knife edge decreased; the latter was situated just above the sample to minimize scattering of the primary beam into the detector. In the worst cases, blocking of this aperture resulted in total loss of signal and a premature end to the experiment.

The work presented in this paper has been carried out on the NdCu, $NdCu_2$, and $NdCu_5$ alloys of neodymium and copper and the $CeCu_2$ alloy. In all cases, the "structure" of the intermetallic precursor is known (*10*). The phases produced during the activation process have, where possible, been assigned by reference to the JCPDS data base (*11*) and the literature. Quantitative analysis of the data has been performed by fitting "pseudo-Voigt" functions to observed diffraction peaks to obtain peak widths (FWHM) and peak intensities.

RESULTS

Before proceeding with a description of the behavior of these systems, a number of points relating to the interpretation of the diffraction and activity data are worthy of note. The presence of copper in the sample and the use of Cu K_α radiation, together with the nature of the sample cell, gives rise to a high background signal. In addition to the consequent deterioration in signal: noise, this has a number of other effects and in particular, it affects the detection limit for minority phases. The situation is also complicated by the very nature of the final phases, namely, poorly crystalline materials giving rise to rather broad, frequently overlapping diffraction peaks.

The analysis and structural assignment of unknown phases is limited by the accuracy to which d values (i.e., lattice spacings) can be determined as a result of

(i) the error in alignment of the high-pressure sample cell with the position-sensitive detector, but *more* importantly, as mentioned earlier, the loss of vertical alignment as the sample expands during the course of the activation;

(ii) the poor crystallinity of many of the phases yielding significant errors in the

peak maxima determination and an absence of well-defined high-angle peaks;

(iii) the absence of a good internal standard.

The low conversions employed should ensure that the qualitative interpretation of the activity data is not unduly influenced by any variation in the flow/diffusion conditions under which the catalyst was operated. Much more significant is the absence of any information on the evolution of active surface area during any particular run and on differences in ultimate surface areas between experiments. The possibility of the temperature of the catalyst bed during activation being significantly greater than the nominal reactor temperature as a result of the exothermicity of the oxidation (*8*) also needs to be considered, although the use of a small charge spread uniformly over an efficient heat sink (the reactor block) and, indeed, the thermal conductivity of high-pressure hydrogen should limit any such effects. Under the gas flow conditions (residence time ~1 min) employed, good gas/surface equilibration is highly likely. X-ray penetration into the loosely packed catalyst bed is substantial, although of course the sampling depth for any individual particle is of the order of μm.

1 : 1 Alloy (NdCu)

The intermetallic compound NdCu has an FeB-type structure (a = 7.279 Å, b = 4.514 Å, c = 5.634 Å (*10*)) and XRD data reveal that within the temperature, gas composition, and pressure regimes studied two modes of behavior may be observed. The following experiments on this system have been carried out:

(i) activation in synthesis gas (syngas, $CO : H_2 = 1 : 2$) at 423 K;

(ii) hydrogen pretreatment at 423 K with subsequent exposure to syngas at this temperature;

(iii) hydrogen pretreatment at 350–373 K with subsequent exposure to syngas at 423 K;

(iv) initial hydrogen treatment at 350–373 K with further heating to 448 K prior to activation in synthesis gas at 423 K.

Figure 2 shows a sequence of diffraction patterns obtained during the activation of NdCu alloy in syngas at 423 K and 15-bar total pressure. They reveal a rapid conversion of the intermetallic to an fcc based structure with lattice parameter characteristic of the nonstoichiometric binary Nd hydride (NdH_{2+x}: $0 \leq x \leq 1$) (trace (c)) with subsequent transformation to a mixture of C-type Nd_2O_3 and Cu crystallites. It should be noted that both the oxide and hydride have structures based on the fluorite lattice with very similar unit cell parameters for the fcc Nd sublattice (*12, 13*). Hence the XRD patterns, dominated by scattering from the Nd atoms, are virtually identical, except that the hydride peaks are shifted, by an amount which increases with the scattering angle, to higher 2θ. This gives rise to the doublet appearance of the rare earth (RE) phase lines in traces (d)–(f).

This assignment has been confirmed by a study of the reactive behavior of the pure binary neodymium hydride. The binary RE hydrides exhibit nonstoichiometry over a wide range of compositions; in the case

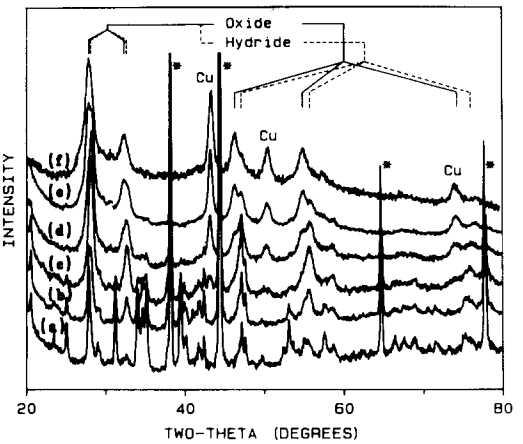

FIG. 2. Synthesis gas activation of NdCu precursor. Increasing vertical offset of the XRD patterns corresponds to increasing exposure (0–18 h) at 15 bar/423 K. (Asterisks indicate the aluminum sample holder.)

of neodymium from $NdH_{1.9}$ to the trihydride, NdH_3, without any change in structure type (*12*). Well crystalline Nd hydride, obtained commercially, was pretreated in hydrogen and then exposed to syngas under increasingly severe conditions (Fig. 3). Perhaps rather surprisingly, the conversion of hydride was observed to occur very slowly even at 15 bar/523 K. Further treatment at this temperature in an ambient pressure of pure oxygen for several hours did not significantly alter the oxide : hydride ratio from which it can be concluded that further oxidation is kinetically inhibited by the formation of an oxide layer. The match between the hydride and oxide of pure neodymium with the peaks obtained during the activation of the 1 : 1 intermetallic is excellent.

A quantitative analysis of the composition as a function of activation time for the alloy precursor (Fig. 4) was obtained by fitting the Cu(111) peak and both the (400) and (440) peaks of the RE hydride/oxide. It confirms the initial rapid formation of the hydride phase with subsequent concurrent growth of Cu and C–Nd_2O_3 crystallites. The appearance of these two phases coincides with the onset of methanol synthesis activity; furthermore, the rise in reaction rate and leveling-off of the methanol yield parallels the growth of the copper and oxide crystallites.

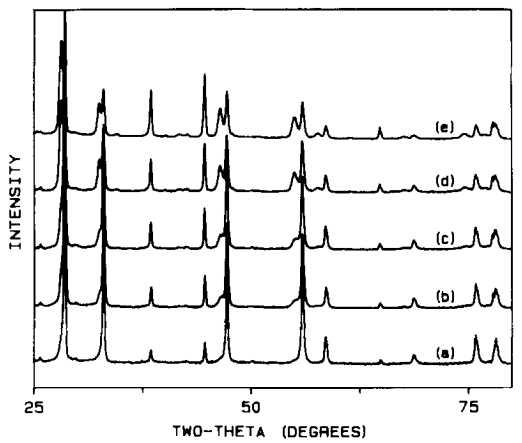

FIG. 3. Oxidation of binary neodymium hydride in a synthesis gas atmosphere (absolute pressure 8 bar unless specified). Exposure time (a) 8 h/423 K; (b) +8 h/498 K; (c) +12 h/498 K; (d) +12 h/523 K; (e) +8 h/15 bar/523 K.

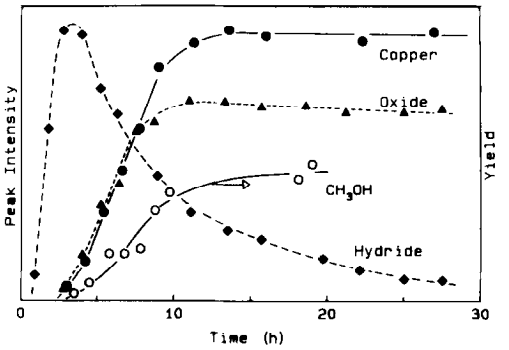

FIG. 4. Structural and activity data (arbitrary units) for synthesis gas activation of NdCu at 15 bar/423 K showing the correlation between the growth of methanol activity and copper/neodymium oxide peak intensities.

The methanol yield from syngas-activated NdCu is relatively low and, as seen in Fig. 2, is associated with relatively well crystalline Nd_2O_3. Pretreatment in pure hydrogen can, under certain conditions, dramatically increase the initial activity obtained and also give rise to a morphologically very different catalyst. If the reactor is pressurized to 15 bar H_2 and the temperature then raised to 423 K over a period of 45 min, then the evolution of the intermetallic is very similar to the initial stages of syngas activation; more specifically, there is the formation of a relatively well crystalline phase with diffraction pattern corresponding to the structure of the binary Nd hydride but virtually no crystalline copper visible even after complete conversion of the initial alloy, a feature which is discussed in more detail later. Changing the feed to a synthesis gas mixture with the reactor maintained at 423 K results in the initiation of methanol synthesis activity, which gradually increases to a limiting value over a period of about 4 h, together with the growth of Cu crystallites and Nd

hydride-to-oxide conversion. However, there is also a very rapid increase in intensity of an additional peak at ~31° 2θ (only weakly present after the H_2 treatment and not observed in the original syngas experiment). Over the 4 h to steady state activity the intensity of this peak then gradually decreases ~40% before reaching a virtually constant value. The nature of the phase giving rise to this peak is more clearly revealed by pretreatment under less vigorous conditions.

If the 1:1 alloy is exposed to the same pressure of hydrogen at lower temperatures (≤373 K) then there is a gradual conversion, not to the binary RE hydride type structure but selectively to a second phase believed to be an *intermetallic hydride* (Fig. 5, trace (b)). An unambiguous assignment of this structure has not yet been made but the complete absence of any Cu-diffraction features and peak widths comparable to those of the initial intermetallic are consistent with this interpretation. Once formed, this phase may be heated to 448 K for several hours yet still only shows slight breakdown to the binary RE hydride structure in a pure H_2 atmosphere. Subsequent exposure of this material to syngas at 423 K gives an extremely rapid activation and accompanying expansion, with very high initial methanol synthesis activity. The rapidity with which this process occurs and the associated massive expansion have prevented a detailed diffraction study of the metamorphosis but the patterns which have been obtained (Fig. 5, traces (c), (d)) indicate that the initial product is essentially X-ray amorphous, with only very broad peaks corresponding to Nd hydride/oxide and residual intermetallic hydride observed and *no* crystalline Cu present. After ~3 h on stream, however, XRD patterns of the *air-discharged* catalyst reveal the presence of relatively large Cu particles ($FWHM_{(111)}$ = 0.56°; *d* (Debye–Scherrer) ~200 Å) in addition to poorly crystalline Nd hydride/oxide and, rather surprisingly in view of its initial reactivity, still a small amount of residual intermetallic hydride.

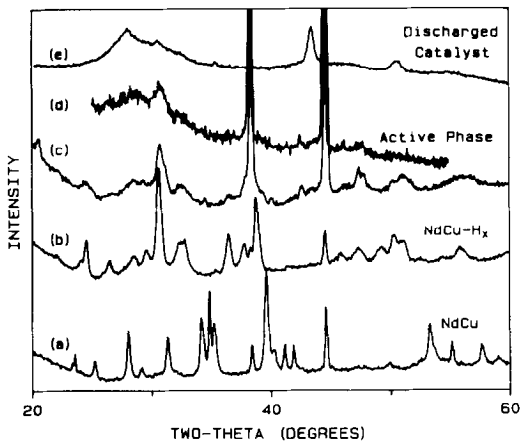

FIG. 5. Synthesis gas activation of low-temperature H_2-pretreated NdCu: (a), (b) Pure H_2 atmosphere, 15 bar/363 K; (b), (d) CO/H_2 atmosphere, 15 bar/423 K; (c), (d) obtained after ca. 30- and 60-min exposure, respectively; (e) air-discharged catalyst.

1:2 Alloys

(*a*) *$NdCu_2$*. The activation of the 1:2 alloy in syngas has been studied by XRD over a wide range of conditions of temperature and pressure but concurrent activity data are only available for activation at 423 K/15 bar. Under these conditions activation takes place over a period of about 6 h. Increasing the temperature significantly reduces this time but does not alter the fundamental behavior observed during the activation process. The sequence of diffraction patterns presented in Fig. 6 were collected at 35-min intervals during activation at 448 K/8 bar. The peaks corresponding to the starting alloy are essentially visible only in the first trace and this transformation of the precursor is accompanied by the rapid growth of a peak at 33° 2θ (trace (b)) representing a transient phase in the activation process. The equally rapid disappearance of this phase is then associated with the growth of peaks apparently corresponding to C–Nd_2O_3 and Cu crystallites. The shift in the peak maxima of the low-angle "oxide" peak to smaller 2θ, however,

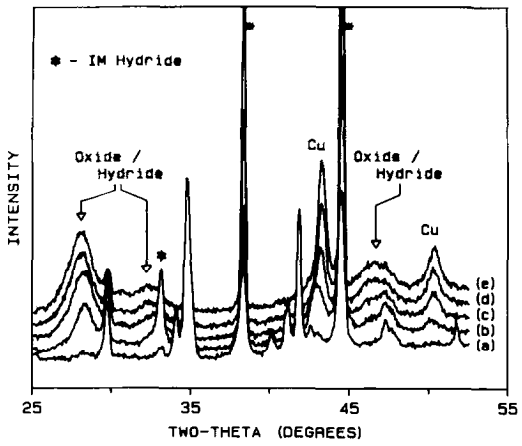

FIG. 6. Synthesis gas activation of $NdCu_2$ precursor. Sequential diffraction patterns obtained at 35-min intervals during treatment at 8 bar/448 K. (a) Corresponds to virtually untransformed starting alloy. (b) Small diffraction features from residual alloy removed for clarity.

suggests that, as observed for the 1 : 1 alloy, a binary Nd hydride-type phase is an intermediate in the decomposition and oxidation of the transient phase.

Since the crystallinity of the two RE phases is lower than that observed during syngas activation of the 1 : 1 alloys, and the peaks are, as a consequence, totally unresolved, it has only been found possible to fit reliably a single function to the observed profile. The variation of integrated intensities of this combined peak and the main peaks of the transient phase and the copper are illustrated in Fig. 7A for activation at 423 K. The peak widths and peak maxima obtained by fitting the experimental data for the low-angle peak reveal (Fig. 7B) a large increase in the FWHM and significant shift in the peak maxima to lower 2θ, virtually concurrent with the growth of the Cu crystallites which, by analogy with the 1 : 1 alloy, is taken to correspond to the onset of hydride-to-oxide conversion. The rise in methanol activity (Fig. 7C) is again seen to correlate with this conversion and the growth of Cu crystallites while the removal of carbon by hydrogen leads to an enhanced methane yield during the oxidation process.

The role of the gaseous components and the nature of the intermediate phases is further elucidated by treatment of the intermetallic precursor in pure hydrogen and pure carbon monoxide. In pure hydrogen at 383 K a metastable, intermetallic hydride, observed also as the "transient phase" in the syngas activation, is rapidly formed. Under the conditions used this compound rapidly and irreversibly decomposes to what is predominantly a Nd hydride-type phase of fcc structure, which is identical, or very similar, to that formed from the 1 : 1

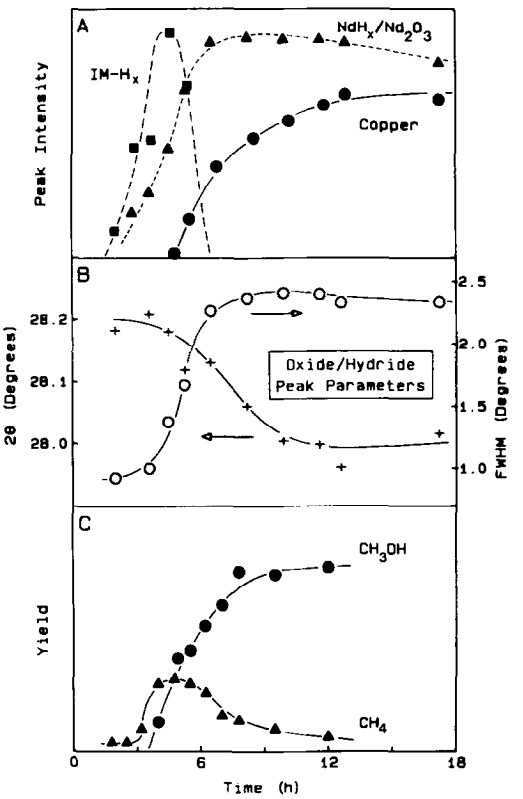

FIG. 7. XRD peak parameters and GC activity data for $NdCu_2$ activation in CO/H_2 at 15 bar/423 K: evolution with reaction time of (A) peak intensities of product phases—transient intermetallic hydride, copper, and unresolved Nd hydride and oxide; (B) combined Nd hydride/oxide (222) peak parameters—peak width (FWHM) and position (2θ); (C) methanol and methane synthesis activity (A,C, arbitrary units).

alloy at 423 K except that it is of rather poorer crystallinity or significantly smaller particle size (Fig. 8). In addition, extra peaks are observed revealing the presence of a significant quantity of yet another hydrided phase, together with very weak and broad peaks at the angles corresponding to pure copper. The hydrogen sorption behavior described is pressure independent over the range 8–30 bar and temperature independent for $T < 408$ K with CO/H_2 experiments suggesting that the temperature invariance extends to over 473 K. Subsequent exposure of this material to syngas results in the expected shift of the RE phase peaks on conversion of hydride to oxide and the growth of large Cu crystallites. By contrast, the $NdCu_2$ alloy is very resistant to chemical change when heated in pure CO ($P_{CO} = 2$ bar), exhibiting only slow and partial oxidation over a period of several hours at 523 K, whereas complete conversion occurs within 5 min under the same conditions in syngas.

Activation studies in syngas at pressures of 2, 8, 15, and 22 bar reveal very few differences of behavior that are of significance. The transient intermetallic hydride was not observed during activation at 2 bar but studies at this pressure have been limited to an activation temperature of 513 K and the metastable nature of this phase means that it becomes increasingly harder to observe by XRD at higher temperatures as its rapid decomposition prevents the buildup of a significant bulk concentration. There is also some indication that the crystallinity of the oxide phase in particular decreases with increasing pressure although this may just reflect the lower temperature at which activation can be initiated.

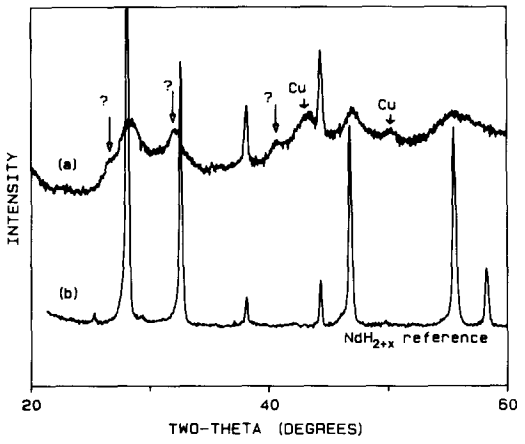

FIG. 8. XRD pattern (a) obtained after extensive treatment of $NdCu_2$ in pure H_2 at temperatures up to 383 K, together with reference pattern; (b) from pure binary neodymium hydride. Peaks due to copper crystallites and additional phase(s) marked accordingly.

The effect of temperature on the crystallinity of the final C–Nd_2O_3 and Cu phases produced has also been studied. In one such experiment, the catalyst was activated in 8 bar of syngas at 448 K for 6 h and the temperature then raised, initially to 503 K for a further 6 h and finally to 573 K for an additional 12 h. During the very early stages of this activation the measured Cu(111) peak width was ~0.8° but after 2 h this decreased rapidly to a value of ~0.6°. Only a very small decrease in this value was observed even after 6 h at 503 K but an increase in the temperature to 573 K resulted in a further rapid decrease to a limiting value of ~0.54°. The final increase in temperature, however, had no observable effect on the measured integrated intensity of the main Cu peak which reached a limiting value after ~5 h at 503 K, having attained 83% of this value after the first 6 h at 448 K. The greater width of the Cu peak, and implied smaller crystallite size, during the very early stages of activation is believed to be a real effect but, since there is overlap with a weak peak of the intermetallic hydride at this point, the derived value may *in part* be an artefact of the fitting procedure.

Analysis of the RE oxide peaks is also complicated by overlap, in this case with the residual Nd hydride peaks. The single-function fit for the activation at 448 K is initially virtually identical to that at 423 K illustrated in Fig. 7, but with the peak width

and integrated intensity reaching a maximum value after ~5½ h. The subsequent increase in temperature to 503 K resulted in a fall in both of these quantities by ~15–20% (for the (222) peak) over a period of 6 h, followed by a further 2–12% decrease during the first 6 h at 573 K, after which only a very slight change was observed. This continued fall in both parameters suggests that complete oxidation of the hydride is not achieved, even within the X-ray sampling depth, for many hours after initial activation.

Activation studies at various temperatures within the range 403–513 K reveal a fairly steady decrease in peak width (for both Cu and Nd_2O_3 phases) with increasing temperature. Although more significant than the variations observed for activation at different pressures but constant temperature, this effect is still small for the Cu crystallites and although apparently larger for the RE oxide phase, much of this may be due to the presence of residual binary hydride at the lower temperatures.

(*b*) *$CeCu_2$*. In many ways the behavior of the $CeCu_2$ intermetallic mirrors that of its Nd counterpart, differing only in the reactivity of the various phases. The first structure (T1) to be observed during activation in syngas or pure hydrogen is isomorphous with the transient phase observed for $NdCu_2$. This transformation may be carried out selectively by exposure to 15 bar CO/H_2 (1 : 2) at 343 K (~6 h) to 373 K (~1 h) (Fig. 9). In the same pressure of pure hydrogen, however, even at 333 K this phase is rapidly formed (~45 min) but interconverts to a second hydrided phase (T2) within a very short time interval.

The ability to form the T1 phase selectively in a relatively well crystalline form has enabled a structural assignment to be made in this instance with the best fit yielding a hexagonal unit cell (a = 4.259 Å, c = 8.197 Å for $P_{CO/2H_2}$ = 15 bar) with the intense line at ~32.75° 2θ corresponding to the (003) reflection. This change can be visualized as an expansion along the y-axis,

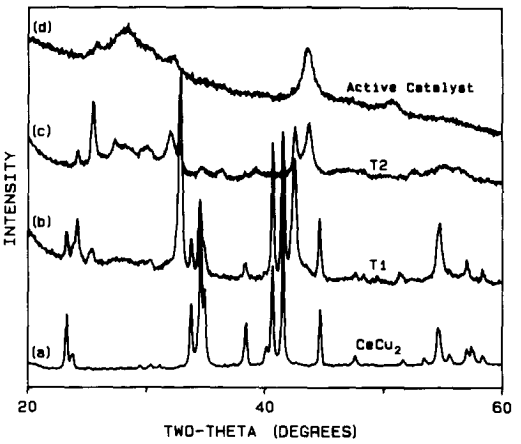

FIG. 9. Synthesis gas activation of $CeCu_2$ precursor (a) starting alloy (He atmosphere)—subsequent diffraction patterns during treatment in 15 bar CO/H_2 at 353 K (b) and 373 K (c,d).

with slight compression along the other two axes of the orthorhombic unit cell (a = 4.43 Å, b = 7.05 Å, c = 7.45 Å (*10*)) of the intermetallic precursor, corresponding to a volume expansion of 10.7% upon hydrogen absorption to form an intermetallic hydride ($CeCu_2$–H_x) of unknown stoichiometry.

The initial hydrogen absorption to form the T1 phase is probably only reversible under very carefully controlled conditions since the T1 → T2 transition occurs readily. This conversion is observed to be very much more facile in pure H_2 as opposed to the same total pressure of syngas. Whether this is merely a reflection of the higher hydrogen partial pressure or represents an inhibiting effect exerted by the presence of CO has yet to be ascertained.

Annealing of the T2 phase in flowing He at 423 K for 2 h gives a mixture of 3 phases, namely, the binary "Ce hydride" phase, a small amount of elemental copper and a third phase which appears to correspond to a contracted T2 phase as might be obtained by a decrease in the absorbed hydrogen content of an intermetallic hydride. There is no indication of a reverse transformation yielding the T1 phase under these conditions. In 15-bar pure hydrogen at 373 K

the T2 phase only exhibits ~50% decomposition to the Ce hydride phase after 10 h exposure, whereas under identical conditions in synthesis gas the conversion is virtually 100% complete (Fig. 9, trace (d)) and, in the later stages, is accompanied by a steady growth of Cu crystallites and a shift in the RE phase peaks (in the case of Ce to higher 2θ) representing the RE hydride-to-oxide conversion.

Although the diffraction pattern exhibited by the oxide produced clearly corresponds to the fluorite structure adopted by CeO_2, it is highly likely that under the reducing conditions of methanol synthesis, the oxide, in addition to being highly defective, is also substoichiometric in oxygen (*15*). There is, however, no evidence for the presence of any of the well characterized lower oxides (Ce_nO_{2n-2} – n = 4, 6(?), 7, 9, 10, 11 (*12*)) in the activated catalyst.

Peak fitting to obtain an accurate quantitative analysis of the composition as a function of time is again complicated by peak overlap, but even more so in this case owing to the presence of the T2 phase. The development of the various phases and the growth of methanol synthesis activity are presented in Fig. 10 for the initial stages of activation in syngas at 373 K: virtually identical behavior was observed for activation at 398 K subsequent to pretreatment in pure H_2. Even after H_2 pretreatment, there is still an induction period of over an hour at 398 K before methanol synthesis is initiated and in both cases the best correlation with the rise in activity is the growth of the Cu and CeO_2 phases. In contrast to the 1 : 1 alloy of neodymium, prior treatment of $CeCu_2$ in pure hydrogen did *not* increase the initial activity; if anything, a slight decrease was observed.

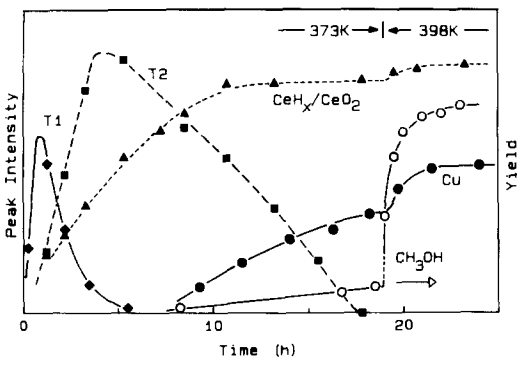

FIG. 10. Combined structural and activity data for synthesis gas activation of $CeCu_2$ at 15 bar/373 K with a subsequent rise to 398 K.

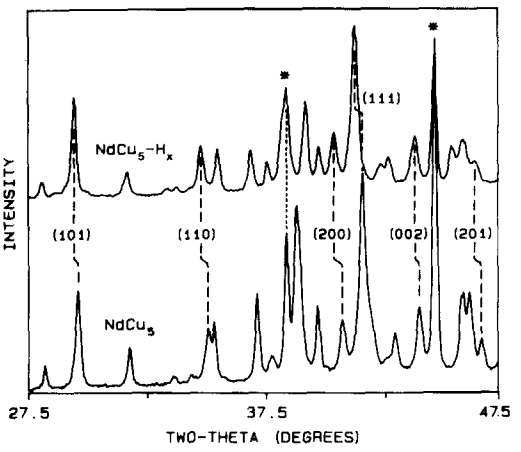

FIG. 11. XRD patterns from as-prepared and hydrided $NdCu_5$ alloy with indexing and reversible peak shifts illustrated. (Additional diffraction peaks correspond to Al-sample holder and 1 : 6 alloy.)

"1 : 5" Alloy ($NdCu_5$)

The prepared sample of nominal stoichiometry $NdCu_5$ was found to be multiphasic, containing, in addition, substantial quantities of $NdCu_6$. The reactive behavior of the two alloys was, however, found to be broadly similar.

The 1 : 5 alloy has the same hexagonal $CaCu_5$-type structure as that exhibited by $LaNi_5$ and many other REM_5 intermetallic compounds whose hydrogen absorption properties have been studied so extensively in recent years. It is easily and reversibly hydrogenated as illustrated in Fig. 11 where the shift in the marked diffraction peaks to lower 2θ represents a virtually isotropic expansion of the lattice by 2.8% on exposure to 30 bar pure H_2 at 373 K. The volume expansion observed for $NdCu_5$

over the pressure range studied here (10–30 bar) is very much lower than that found in most other 1:5 systems. Studies of the $LaNi_{5-x}Cu_x$ (*16*) and $CeNi_{5-x}Cu_x$ (*17*) systems have shown that the hydrogen absorption capacity decreases and the hydride stability increases as Ni is replaced by Cu. The decrease in hydrogen absorption capacity does not, however, seem to be reflected in the lattice expansion which remains virtually constant at ~15% for $2 \leq x \leq 4$ in the Ce(Ni, Cu) system. In addition, the work of Kuijpers (*18*) on the $RENi_5$ and $RECo_5$ systems reveals an increase in the dissociation pressure in the series La–Pr–Nd–Sm and, for the Co intermetallics at least, a small fall in the hydrogen absorption capacity with a virtually constant fractional volume expansion per adsorbed mole of hydrogen. The observed 2–3% expansion is, therefore, surprisingly small for formation of an intermetallic hydride, yet too large to be explained by the formation of a limited solid solution of hydrogen; i.e., the precursor state to ternary hydride formation. A single cycle of hydrogen absorption/desorption may be accomplished without any appreciable loss in intensity and/or broadening of the intermetallic lines and the thermal stability of the intermetallic hydride with respect to hydrogenolysis (decomposition to binary RE hydride and transition metal) is high in that even after 12 h at 473 K in 30 bar H_2 the extent of breakdown is small (<10%).

This same intermetallic hydride is observed during the initial stages of activation in syngas (P_{H_2} = 10 bar). However, the stability of this hydride, as mentioned above, is such that it is essentially inert to further reaction below 473 K. At higher temperatures the intermetallic hydride does gradually decompose, a process complete after ~16 h at 503 K (Fig. 12), with some evidence even in this case for an intermediate Nd hydride phase which is, however, relatively rapidly oxidized under these conditions. The high stability of the intermetallic hydride to both hydrogenolysis and

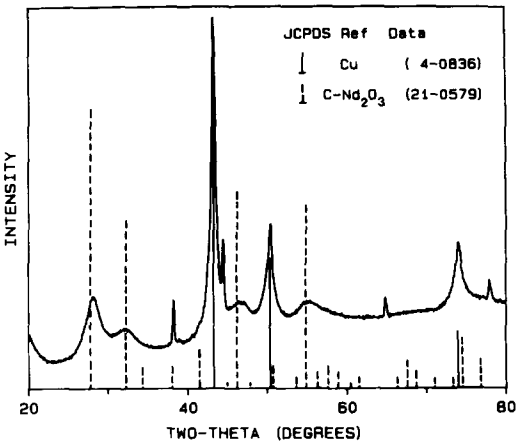

FIG. 12. XRD pattern from a fully "activated" $NdCu_5$ sample (reference patterns from JCPDS data base (*11*)).

oxidation is probably caused by the limited extent of hydrogen absorption. Consequently, high temperatures are required to break down the lattice and copper expulsion from the matrix gives rise to some very large crystallites. It is worth noting that the intermetallic compound contains sheets of pseudo-close-packed copper atoms running through the structure and the failure to disrupt this arrangement by hydrogen absorption means that there is present a natural precursor to large Cu crystallites.

The activity of the catalyst is observed to rise steadily over the first 6 h at 503 K and then rather more slowly for the next 8 h. The steady state activity, even at this elevated temperature, is, however, *very* much lower than that observed for the lower copper content catalysts. Pretreatment in pure hydrogen to form the intermetallic hydride prior to the activation in syngas has very little effect either on the rate at which synthesis activity is attained or on the actual magnitude of the steady state activity.

The diffraction pattern of the fully activated catalyst (Fig. 12) is consistent with the presence of only two phases (elemental copper and C-type Nd_2O_3) but the following points are noted:

(i) the lineshape of the Cu peaks is significantly more Lorentzian than usually observed and suggests a bi- (or poly-) modal distribution of Cu crystallite sizes;

(ii) the Cu peak positions are in very good agreement with the JCPDS reference pattern but the neodymium oxide peaks are shifted fractionally to higher angles, i.e., corresponding to a slight lattice contraction (all peak positions measured at ~300 K).

The unusual Cu lineshape means that the FWHM obtained by fitting does not accurately reflect the mean particle size but, in view of the very low activity exhibited by these catalysts and the inherent problems with profile analysis, this feature was not pursued any further.

In addition, the discharged catalyst is visually different from the lower Cu content catalysts in that it is of a "salmon pink" color characteristic of a dispersion of relatively large copper particles.

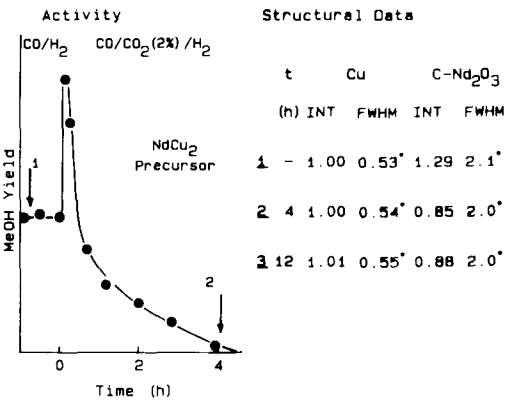

FIG. 13. Effect of CO_2 on the activity and composition of a catalyst prepared from an $NdCu_2$ intermetallic precursor. Activity data: evolution of methanol yield with time. Structural data: variation of fitted peak parameters (intensity and width of the Cu(111) and C–Nd_2O_3 (222) peaks) with time (t) after the switch in feed gases.

Structural Effects on CO_2 Poisoning

The effects of CO_2 poisoning on intermetallic derived catalysts (*6*, *8*) have been studied by switching the feed gas to an activated $NdCu_2$ catalyst from pure syngas to a mixture of syngas incorporating 2% CO_2. This was carried out at a constant temperature and pressure of 473 K and 15 bar, respectively, following activation at 423 K and subsequent stabilization at 473 K. Under these conditions, the change in feed gas results in a transient peak in the methanol yield (Fig. 13) and then a rapid fall to essentially zero activity. A return to the original CO_2-free feed mixture does not result in any regeneration of activity, showing the poisoning to be an irreversible effect.

Prior to the change in feed gas the only phases visible by XRD were Cu and C–Nd_2O_3. The measured changes in integrated peak intensity and peak width for these two phases on exposure to the CO_2-containing syngas are given in Fig. 13. Both phases exhibit small changes in the width of the diffraction peaks which may or may not be real effects. The intensity of the Cu peaks shows no change whatsoever but the intensity of the Nd_2O_3 peaks falls significantly (~33%) while the activity is decreasing and then levels off at a lower value. No new weak diffraction features are observed after this treatment.

The substantial variations in activity displayed upon switching to a CO_2-containing feed gas do not, therefore, appear to correspond to any significant changes in the bulk composition of the active catalyst. The presence of CO_2 is known to influence the oxidation state of the Cu crystallites (*19*), but it might also be expected that the basic RE oxides would form a carbonate or oxycarbonate under such conditions. The limited XRD evidence available does not contradict this idea; indeed, the loss of intensity of the RE oxide peaks could be attributed to the formation of a surface coating of another phase. The failure to observe new XRD peaks does mean, however, that any such additional phase must be sufficiently disordered or of limited size in at least one dimension (e.g., thickness) with the result that any diffraction features are lost in the background.

DISCUSSION

The proposed behavior of the intermetallic systems studied is summarized in Fig. 14. In all cases, except perhaps the 1:5 alloy, a phase hitherto referred to as having a "binary RE hydride" structure is seen to play an important role. The exact nature of this phase therefore warrants further discussion. A true binary hydride may be formed from a RE–TM intermetallic compound on exposure to hydrogen either by complete hydrogenolysis, yielding additionally the second metallic component in elemental form, or by disproportionation to RE hydride and an intermetallic hydride enriched in the TM component. In neither the 1:1 nor the 1:2 alloys studied here is disproportionation believed to occur, there being no evidence for the presence of a Cu-enriched intermetallic hydride. Complete hydrogenolysis involves a severe disruption of the initial lattice as the transition metal is expelled from the matrix; by contrast, hydrogen absorption yielding an intermetallic hydride may occur with negligible disruption.

The effect of substantial lattice restructuring is clearly evident in the diffraction patterns, particularly so for the 1:2 alloys, with the half-widths for the hydride structures being significantly greater than for the parent compound. Rather surprising, however, is the intensity of the Cu peaks obtained in pure hydrogen, which, even allowing for their substantial breadth, is very low, especially for the 1:1 alloys. The observation of these weak Cu diffraction

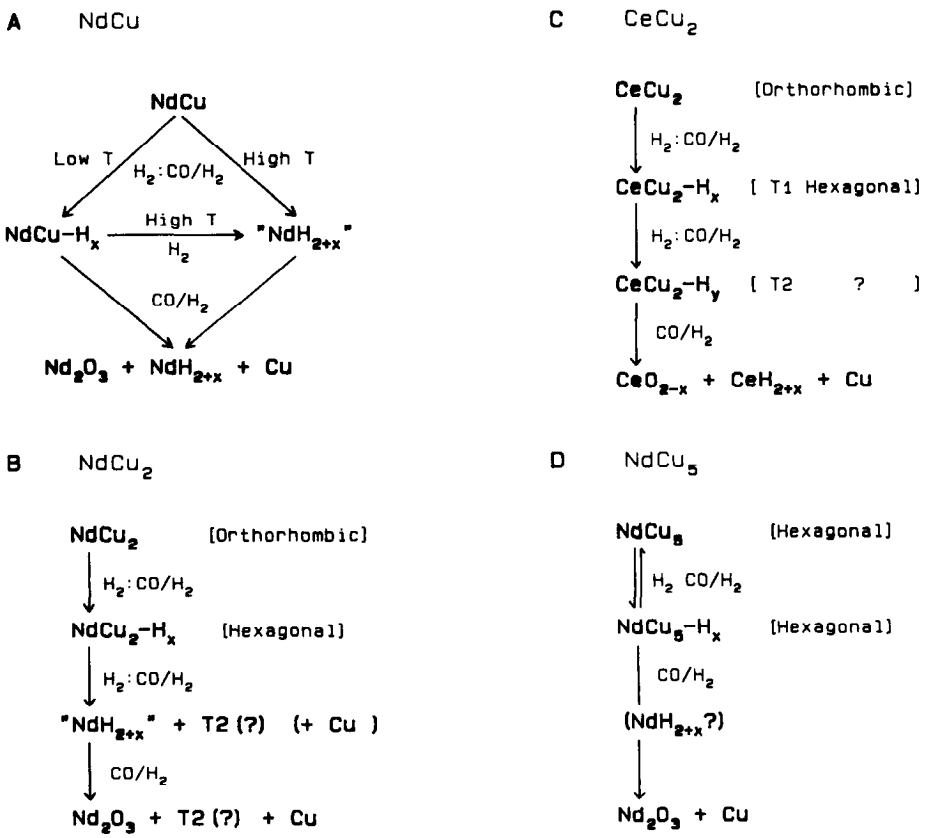

FIG. 14. Summary of activation behavior: the role of intermediate phases in the conversion of alloy precursors to final catalyst.

lines does show that at least some of the Cu atoms have been expelled from the matrix; what is less certain is whether the remaining "invisible" Cu is present as highly dispersed clusters or thin layers of elemental Cu on the surface of the hydride of a sufficiently small size not to be revealed by the XRD or whether, as suggested by Semenenko and Burnasheva (*20*), substantial quantities may remain within the "RE hydride" lattice. Furthermore, in this latter case, the Cu could in principle be present either interstitially, atomically dispersed or as small cluster defects, or substitutionally in the framework.

It is certainly the case that substantially more elemental Cu is observed at lower temperatures following hydrogenolysis of the more Cu-rich 1 : 2 alloys, but neither this nor the observation of concurrent growth of Cu and C–Nd_2O_3 in a number of experiments allow one to differentiate with certainty between these two possibilities. The concurrent growth of the two phases does, however, strongly suggest that the sintering mechanism giving rise to the "large" Cu crystallites is directly associated with the oxidation process and that the nominally binary hydride may well incorporate, in one form or another, substantial quantities of copper to the extent only that it is substoichiometric in copper relative to the 1 : 1 alloy.

The evidence for the reactive behavior of the NdCu intermetallic precursor summarized in Fig. 14A will now be considered. The least activated interaction of the alloy with a hydrogen atmosphere is observed to be formation of an ordered intermetallic hydride. This intermetallic hydride is stable to temperatures higher than those at which the "binary Nd hydride" is preferentially formed from the parent intermetallic, so a direct route of alloy hydrogenolysis must exist. The observed switch in alloy reactivity is explicable in terms of a rate inversion for the two processes; the reaction of lowest activation energy dominates below 373 K while at higher temperatures, the entropically favored hydrogenolysis with a high pre-exponential factor becomes increasingly important.

It is of interest to note that the Nd-substructure of the 1 : 1 alloy is in fact easily deformed to give an fcc lattice characteristic of the Nd hydride (Fig. 15), and this may be one reason for the higher crystallinity of the Nd hydride derived from the 1 : 1 as opposed to the 1 : 2 alloy. (The greater amount of Cu that has to be ex-

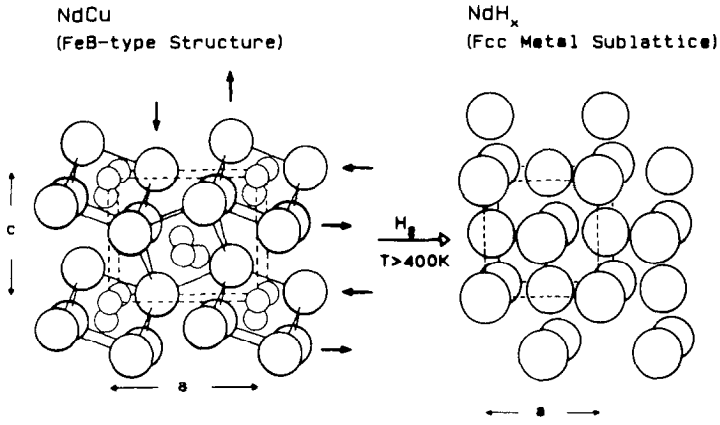

FIG. 15. Crystal structure models showing the close relationship between the Nd sublattice in the 1 : 1 alloy, NdCu, and the binary hydride, NdH_{2+x}. Solid arrows indicate the required atomic displacements to accomplish the transformation. (From Pearson (*21*). Copyright © 1972; Wiley–Interscience. Reprinted by permission of Wiley.)

pelled from the matrix in the latter case will clearly also be a contributing factor.) At temperatures exceeding 448 K decomposition of the intermetallic hydride to yield the Nd hydride is indeed observed as would be expected on thermodynamic grounds. This probably occurs via a direct route rather than by the intermediacy of the original intermetallic.

Exposure of the intermetallic hydride to CO/H_2 at 423 K (i.e., below the decomposition temperature in pure hydrogen) leads to an extremely rapid oxidation/activation that clearly cannot be via the binary hydride which activates at a much slower rate and yields a significantly less active catalyst.

One experimental observation is apparently inconsistent with the scheme outlined above and that is the effect of switching to a syngas feed after high-temperature treatment of the 1 : 1 alloy in pure hydrogen to form the Nd hydride. The resulting unexpected increase in intensity of the previously inconsequential intermetallic hydride peaks could represent a real partial conversion of the binary to intermetallic hydride, i.e., reverse "hydrogenolysis," in which case this would be strong evidence for the incorporation of a relatively high copper content in the supposedly binary hydride, or, perhaps more likely, it is the result of exposure of material previously below the sampling depth by decrepitation of the surface layers during oxidation.

A comparison of the behavior of the neodymium and cerium 1 : 2 intermetallic compounds reveals many similarities. Based on the assignment of a hexagonal unit cell to the T1 phase, $CeCu_2$–H_x, unit cell parameters may be determined for the analogous transient phase formed from $NdCu_2$. The mean values obtained over a hydrogen partial pressure range of 5–30 bar are $a = 4.21$ Å, $c = 8.12$ Å, corresponding to a volume expansion of 9.5% in this case. The orthorhombic $CeCu_2$ structure (the structure also adopted by the $NdCu_2$ intermetallic) may be regarded as a distortion of the hexagonal AlB_2-type structure (*21*) and it seems probable, therefore, that the intermetallic hydride has a bimetallic sublattice of this form.

What this work shows quite clearly is that in the case of cerium, the second transient phase is an intermediate in the hydrogenolysis, i.e., there is a sequential conversion through the two intermetallic hydrides, T1 and T2, prior to decomposition to Ce hydride. On first sight, this is not the case with $NdCu_2$ where the T1 phase apparently undergoes rapid and direct hydrogenolysis. There is, however, a distinct similarity between the T2 phase of $CeCu_2$ and the extra peaks in the XRD pattern obtained after treatment of $NdCu_2$ in pure hydrogen (see Fig. 8) which suggests that there is probably no fundamental difference in behavior, but merely significant variations in the controlling kinetics. The complete breakdown of the lattice is definitely less favored in the case of cerium, hence allowing the formation of the T2 phase with high selectivity. The difference may be attributed to a higher free energy of formation of the intermetallic hydride than for neodymium and, consequently, a greater activation energy for decomposition.

Table 1 summarizes concurrently obtained structural and activity data for all the alloys studied, following various activation procedures. If it is assumed that all the copper present in the intermetallic precursor is ultimately converted to crystallites of a size given by the application of the Debye–Scherrer equation to the elemental Cu diffraction peaks (~200 Å), then the Cu surface area of the activated $NdCu_2$ catalyst cannot exceed ~20 $m^2\ g^{-1}$. The complete absence of methanol synthesis from a $CO/CO_2/H_2$ feed at 473 K/15 bar shows that the mechanism proposed by various authors (*22, 23*) for methanol synthesis from CO_2 on the copper component of the commercial $Cu–ZnO/Al_2O_3$ catalyst is not applicable to these alloy-derived catalysts. This

TABLE 1

Summary of Catalytic and Structural Data

Precursor	H_2[a]	Activity[b]		Structural data[c]		
		Temp. (K)	Yield (arb. units)	Int. ratio Cu/Nd_2O_3	FWHM	
					Cu	Nd_2O_3
$CeCu_2$	—	398	375	0.80	0.74°	2.5°
	LT	398	310	0.51	0.73°	1.9°
NdCu	—	423	115	0.49	0.69°	1.2°
	HT	423	650	0.20	1.00°	2.5°
	LT	423	2940	[0.24	0.56°	2.7°][d]
$NdCu_2$	—	423	410	0.59	0.54°	2.2°
$NdCu_5$	—	503	35	1.61	~0.62°	2.0°
	HT	523	135	1.45	~0.64°	2.2°

[a] Hydrogen pretreatment (P = 15 bar) at 350–373 K (LT) or 423–523 K (HT) prior to activation in synthesis gas.

[b] Activity data (arb. units) measured in $CO/2H_2$ (P = 15 bar) at the specified temperature and normalized to unit mass of discharged catalyst assuming a linear methanol yield/catalyst charge relationship.

[c] Structural data presented as the ratio of integrated intensities for the Cu(111) and C–Nd_2O_3(222) peaks: peak widths (FWHM) also shown.

[d] Peak parameters only available for the air-discharged sample owing to massive expansion (during the early stages of activation this catalyst was virtually X-ray amorphous).

is a major conclusion of the present paper and has been confirmed by radiotracer studies which show no transfer of β-activity from $^{14}CO_2$ into methanol produced following a change in feed gas (*8*). The low-temperature methanol synthesis observed over these intermetallic derived catalysts must therefore be accounted for in terms of CO hydrogenation.

The complete absence of a correlation between the methanol yield and FWHM of the Cu(111) peak or, indeed, any estimate of the elemental Cu surface area made from the XRD data, strongly suggests that the Cu particles *visible* in the XRD are not responsible for the high activity. Support for this conclusion can be drawn from numerous studies of the kinetics of CO hydrogenation over various forms of elemental copper (*24–26*) which would all predict rates orders of magnitude lower than those observed at the conditions used and for the surface area mentioned above.

The only other phase that can be uniquely identified in all the activated catalysts is the RE oxide. Synthesis of methanol over both ThO_2 (*27*) and ZrO_2 (*28, 29*) has been reported in the literature. The former case involved very high surface area samples at temperatures substantially higher than those utilized in this work; in the latter case methanol formation was detected at ~398 K, but this was under transient (TPD) conditions rather than under steady state catalytic conditions. Neither the C–Nd_2O_3 prepared by *in situ* oxidation of neodymium hydride in syngas nor activated Ag–RE intermetallic compounds (*6*), however, show any activity for methanol synthesis at temperatures below 523 K.

There does, nevertheless, appear to be a correlation between the rise in methanol activity and the appearance of either the RE oxide phase or the "large" Cu crystallites. In view of what has already been said,

there seem to remain two possible sources for the high activity:

(i) the interfacial region of the visible Cu crystallites with the RE oxide phase, or

(ii) "very highly dispersed" Cu present on, or within, the surface of the RE oxide.

If a spillover mechanism is in operation, then this distinction may be more apparent than real, but in the latter case, the electronic properties of the copper could differ significantly from those of bulk copper in addition to possible variations in oxidation state and morphology.

Quite high loadings of both Ag and Cu atomically dispersed in RE oxides have been achieved by conventional methods of catalyst preparation (*30, 31*). The noble metal is believed to be present substitutionally in the lattice as the divalent ion and various "active oxygen species" were observed on the Ag-modified oxides following oxygen chemisorption, leading the authors to suggest that these materials are potentially important olefin epoxidation catalysts. The preparation techniques utilized, however, were standard wet chemical procedures, similar to those used by other groups to produce RE-oxide-supported copper catalysts which exhibit only low activity for methanol synthesis (*3, 4, 6*).

Highly dispersed "clusters" of zerovalent copper supported on the oxide would tend to imply a high Cu surface area, in contradiction to the *in situ* N_2O measurements (*6*) that reveal very low metal areas of $\sim 1\ m^2\ g^{-1}$, probably attributable to the large Cu crystallites alone. A very intimate contact with the RE oxide, such as, e.g., very small clusters of Cu embedded within and coordinated to the oxide matrix might, however, give a form of Cu that is unreactive with respect to N_2O decomposition under the conditions employed.

The various hydrides observed during activation clearly play a crucial role in the low temperature activation of these catalysts. Formation of an intermetallic hydride is accompanied by lattice expansion and, presumably, a general weakening of the metal–metal interactions. This in itself facilitates oxidation as can be seen with the 1 : 1 alloy after low-temperature pretreatment in hydrogen. The extent of hydrogen absorption and lattice expansion appears to be critical. $NdCu_5$, e.g., readily absorbs hydrogen, but the resulting structural distortion appears to be insufficient to have a significant effect on the reactivity. On the other hand, some intermetallic hydrides whose formation involves a greater volume expansion exhibit instability and are susceptible to hydrogenolysis; i.e., decomposition to the RE hydride phase prior to any substantial oxidation. It is interesting to speculate as to whether this process is beneficial or actually detrimental to the eventual activity. There is some circumstantial evidence for the latter, namely, the variation of activity of the 1 : 1 catalysts with pretreatment and the higher activity of catalysts derived from $CeCu_2$ as opposed to $NdCu_2$ precursors. The ability of the hydride to readily release hydrogen which can then remove active carbon formed as a by-product of the oxidation reaction, hence preventing the buildup of carbonaceous deposits, may also be important.

In addition to their role in the activation process, there is also the question as to whether residual hydrides have any effect on the steady state activity; in particular, whether they might act as reservoirs of atomic hydrogen, with spillover onto the active phase occurring by diffusion. This would be more likely to occur from remaining intermetallic hydride rather than any binary RE hydride and merits further study. It is certainly the case that some intermetallic hydrides can remain in the catalyst for many hours after the initial activation process and the experiments carried out on pure Nd hydride suggest that significant quantities of that phase will also be present for a substantial period after the onset of oxidation.

CONCLUSIONS

1. Decomposition of Nd/Cu and Ce/Cu intermetallic precursors to yield highly active methanol synthesis catalysts occurs via

intermediate hydride phases. Both intermetallic and rare earth hydrides are involved.

2. Ultimate performance varies widely and depends on the structure and stoichiometry of the precursor. The nature of the interaction of the alloy precursor with gaseous hydrogen and the stability of the stability of the corresponding intermetallic hydride appear to be crucial to the subsequent activation of the catalyst. Furthermore, in certain cases optimum activation cannot be achieved by the use of CO/H_2 mixtures alone.

3. The majority phases in the active catalyst are the rare earth sesquioxide or dioxide and metallic copper. Some rare earth or intermetallic hydride is often also present, and in the most active catalysts, no crystalline copper was initially detectable by XRD.

4. During activation, there is a good correlation between the rise in methanol activity and the growth of rare earth oxide and Cu crystallites, suggesting that the active site is indeed associated with one or both of these phases. *There is, however, no correlation between Cu crystallite size and catalyst activity.*

5. CO_2 is a very effective poison of these catalysts. The major structural effect associated with this phenomenon is a decrease in the intensity of the rare earth oxide diffraction features with no evidence for sintering of the *visible* Cu crystallites.

6. The special activity of these catalysts is *not* associated with the Cu crystallites visible by XRD. It may very well be related to the presence of a more intimate interaction of copper atoms with the oxide phase; this feature is directly attributable to the atomic scale mixing which is present in the alloy precursor.

ACKNOWLEDGMENTS

Financial support under a Joint Research Scheme funded by ICI PLC is gratefully acknowledged. One of us (T.R.) thanks the Science and Engineering Research Council for provision of equipment under Grant GR/D25019. We thank Johnson Matthey Ltd. for a loan of precious metals.

REFERENCES

1. Tennakoon, D. T. B., Schlogl, R., Rayment, T., Klinowski, J., and Thomas, J. M., *Clay Minerals* **18,** 357 (1983).
2. Rayment, T., Schlogl, R., Thomas, J. M., and Ertl, G., *Nature* **315,** 311 (1985).
3. Wallace, W. E., France, J., and Shamsi, A., *in* "Rare Earths in Modern Science and Technology," Vol. 3, Plenum, New York, 1982.
4. Baglin, E. G., Atkinson, G. B., and Nicks, L. J., *Ind. Eng. Chem. Prod. Res. Dev.* **20,** 87 (1981).
5. Daly, F. P., *J. Catal.* **89,** 131 (1984).
6. Jennings, J. R., Lambert, R. M., Nix, R. M., and Owen, G., *Appl. Catal.*, in press.
7. Jennings, J. R., Lambert, R. M., Nix, R. M., and Owen, G., submitted.
8. Jennings, J. R., Lambert, R. M., Nix, R. M., and Owen, G., in preparation.
9. Rayment, T., in preparation.
10. Carnasciali, M. M., Costa, G. A., and Francheschi, E. A., *Gazz. Chim. Ital.* **113,** 239 (1983).
11. JCPDS—International Centre for Diffraction Data (Swarthmore, PA 19081, U.S.A.).
12. Eyring, L., *in* "Handbook on the Physics and Chemistry of Rare Earths" (K. A. Gschneidner, Jr., and L. Eyring, Eds.), Vol. 3, p. 337. North-Holland, Amsterdam, 1979.
13. Libowitz, G. G., and Maeland, A. J., *in* "Handbook on the Physics and Chemistry of Rare Earths" (K. A. Gschneidner, Jr., and L. Eyring, Eds.), Vol. 3, pp. 299. North-Holland, Amsterdam, 1979.
14. Pebler, A., and Wallace, W. E., *J. Phys. Chem.* **66,** 148 (1962).
15. Sørensen, O. T., *J. Solid State Chem.* **18,** 217 (1976).
16. Shinar, J., Shaltiel, D., Davidov, D., and Grayevsky, A., *J. Less-Common Met.* **60,** 209 (1978).
17. Pourarian, F., and Wallace, W. E., *J. Less-Common Met.* **87,** 275 (1982).
18. Kuijpers, F., *Philips Res. Rep. Suppl.* **28,** 1 (1973).
19. Chinchen, G. C., and Waugh, K. C., *J. Catal.* **97,** 280 (1986).
20. Semenenko, K. N., and Burnasheva, V. V., *J. Less-Common Met.* **105,** 1 (1985).
21. Pearson, W. B., "The Crystal Chemistry and Physics of Metals and Alloys." Wiley-Interscience, New York, 1972.
22. Chinchen, G. C., Denny, P. J., Parker, D. G., Short, G. D., Spencer, M. S., Waugh, K. C., and Whan, D. A., Prepr. Pap., *ACS Div. Fuel Chem.* **29,** 178 (1984).
23. Rozovskii, A., Ya., Lim, G., Liberov, L. B., Slivinskii, E. V., Loktev, S. M., Kagan, Yu. B., and Bashkirov, A. N., *Kinet. Catal.* **18,** 691 (1977).
24. Denise, B., Sneedon, R. P. A., and Hamon, C., *J. Mol. Catal.* **17,** 359 (1982).

25. Thivolle-Cazat, J., Bardet, R., and Tranbouze, Y., Prepr. Pap., *ACS Div. Fuel Chem.* **29,** 189 (1984).

26. Liu, G., Willcox, D., Garland, M., and Kung, H. H., *J. Catal.* **90,** 139 (1984).

27. Maj, J., Colmenares, C. A., and Somorjai, G. A., *Appl. Catal.* **10,** 313 (1984); *J. Catal.* **95,** 385 (1985).

28. Ming-Yuan He, White, J. M., and Ekerdt, J. G., *J. Catal.* **90,** 17 (1984).

29. Ming-Yuan He, and Ekerdt, J. G., *J. Mol. Catal.* **30,** 415 (1985).

30. Bobolev, A. V., Loginov, A. Yu., and Vydrin, S. N., *React. Kinet. Catal. Lett.* **29,** 159 (1985).

31. Vydrin, S. N., Loginov, A. Yu., and Bobolev, A. V., *Izv. Akad. Nauk SSSR, Ser. Khim.* **3,** 528 (1985).